



# Conidial heat resistance of various strains of the food spoilage fungus *Paecilomyces variotii* correlates with mean spore size, spore shape and size distribution



Tom van den Brule<sup>a,b</sup>, Cheuk Lam Sherlin Lee<sup>b</sup>, Jos Houbraeken<sup>a,b</sup>, Pieter-Jan Haas<sup>c</sup>, Han Wösten<sup>a,d</sup>, Jan Dijksterhuis<sup>a,b,\*</sup>

<sup>a</sup> TüFN, P.O. Box 557, 6700 AN Wageningen, the Netherlands

<sup>b</sup> Westerdijk Fungal Biodiversity Institute, Applied & Industrial Mycology, Uppsalalaan 8, 3584 CT Utrecht, the Netherlands

<sup>c</sup> Department of Medical Microbiology, University Medical Center Utrecht, Utrecht, the Netherlands

<sup>d</sup> Utrecht University, Microbiology, Padualaan 8, 3584 CH Utrecht, the Netherlands

## ARTICLE INFO

### Keywords:

Fungal spores  
Heat resistance  
Strain variability  
Light microscopy  
Scanning electron microscopy  
Coulter counter  
Flow cytometry  
Spore size  
Spore shape  
Population distribution

## ABSTRACT

Contamination by spores is often the cause of fungal food spoilage. Some distinct strains of the food spoilage fungus *Paecilomyces variotii* are able to produce airborne conidia that are more heat-resistant than similar species. These ellipsoid asexual spores can vary in size between strains, but also within strains. Here, we compared four measurement techniques to measure conidia size and distribution of five heat-sensitive and five heat-resistant *P. variotii* strains. Light microscopy (LM), Scanning Electron Microscopy (SEM) and Coulter Counter (CC) were used to measure and compare the spherical equivalent diameter, while CC and flow cytometry were used to study spore size distributions. The flow cytometry data was useful to study spore size distributions, but only relative spore sizes were obtained. There was no statistic difference between the method used of spore size measurement between LM, SEM and CC, but spore size was significantly different between strains with a 2.4-fold volume difference between the extremes. Various size distribution and shape parameters were correlated with conidial heat resistance. We found significant correlations in mean spore size, aspect ratio, roundness and skewness in relation to heat resistance, which suggests that these parameters are indicative for the conidial heat resistance of a *P. variotii* strain.

## 1. Introduction

Fungal spores are main vehicles for distribution of filamentous ascomycetous fungi in space via water, air and other vectors, or in time as dormant stress-resistant ascospores (sexual spores) in fruiting bodies (Wyatt, Wosten, & Dijksterhuis, 2013). Both types of spores can cause food spoilage; either by conidia (asexual spores) through aerial or other contamination, or by ascospores through surviving heat treatments (dos Santos, Samapundo, Biyikli, Van Impe, Akkermans, Höfte, & Devlieghere, 2018). Reduction of fungal food spoilage becomes an increased priority with a growing world population. Besides, new trends in food industry will put more pressure on the shelf life of processed food and drinks (Leyva Salas, Mounier, Valence, Coton, Thierry, & Coton, 2017). These include shorter heat inactivation treatments and a reduction in the concentration of compounds that counteract the development of microbes like salt, sugar and preservatives. For example,

decrease of heat treatment leads to a better retainment of organoleptic characteristic of the product, as well as less damage of healthy components like vitamins. However, these developments make processed foods and drinks more prone to fungal spoilage.

Fungal spores are an important hallmark for identification of fungal species (Pitt & Hocking, 2009; Samson, Houbraeken, Thrane, Frisvad, & Andersen, 2019). Even after the development of DNA sequencing, spore shape, size, and ornamentation are still significant morphological characteristics for polyphasic taxonomy. In many species descriptions, the spore size is described and differences do occur between closely related species. For example, the black *Aspergilli* *A. niger* and *A. carbonarius* produce conidia with a diameter of 3.5–4.5  $\mu\text{m}$  and 7–9  $\mu\text{m}$ , respectively (Samson, Houbraeken, Thrane, Frisvad, & Andersen, 2019). In addition, the shape of spores is variable between species, ranging from globose *Penicillium roqueforti* conidia to very complex topologies like the star shaped ascospores of *Aspergillus miraensis* (Chen, Frisvad,

\* Corresponding author at: Applied & Industrial Mycology, Westerdijk Fungal Biodiversity Institute, Uppsalalaan 8, 3584 CT Utrecht, the Netherlands.  
E-mail address: [j.dijksterhuis@wi.knaw.nl](mailto:j.dijksterhuis@wi.knaw.nl) (J. Dijksterhuis).

Sun, Varga, Kocsubé, Dijksterhuis, & Samson, 2016; Punt, van den Brule, Teertstra, Dijksterhuis, den Besten, Ohm, & Wösten, 2020).

Conidia of the fungal genera *Aspergillus*, *Penicillium* and *Cladosporium* are predominant in air, as these fungi can form millions to billions of conidia per colony (Andersen, Frisvad, Søndergaard, Rasmussen, & Larsen, 2011; Segers, van Laarhoven, Huinink, Adan, Wösten, & Dijksterhuis, 2016; Ulevičius, Pečiulytė, Lugauskas, & Andriejauskienė, 2004). Conidia are moderately heat-tolerant, with D-values (log reduction time) of 5 min between roughly 55 °C and 64 °C (Punt, van den Brule, Teertstra, Dijksterhuis, den Besten, Ohm, & Wösten, 2020; van den Brule, Punt, Teertstra, Houbraken, Wösten, & Dijksterhuis, 2020; Wyatt, Wosten, & Dijksterhuis, 2013). For food industry, it is of importance to assess the contamination risk of these spores. Therefore, not only the average resistance of conidia to heat or other treatment is of importance, but also the variability of resistance within a colony or between strains is of high importance. Only recently, the topic of spore heterogeneity has been addressed (Geoghegan, Stratford, Bromley, Archer, & Avery, 2020; Punt, van den Brule, Teertstra, Dijksterhuis, den Besten, Ohm, & Wösten, 2020; van den Brule, Punt, Teertstra, Houbraken, Wösten, & Dijksterhuis, 2020).

Historically, fungal spore size is measured using light microscopy (LM) (Samson, Houbraken, Thrane, Frisvad, & Andersen, 2019). Unless using Nomarski filters, a diffraction halo around the spores can lead to a bias in the measurements (Hitchins, Kahn, & Slepecky, 1968). Cryo Scanning Electron Microscopy (cryo-SEM) is a technique often used to study detailed ornamentation of fungal spores and other structures (Staugaard, Samson, & Van der Horst, 1990; van Veluw, Teertstra, de Bekker, Vinck, van Beek, Muller, & Wösten, 2013). Since samples remain hydrated, delicate fungal structures and spores remain their integrity and shrinkage of spores is prevented (Aldrich & Todd, 1986). In addition, this technique does not cause a halo around the spores. Coulter counter (CC) and flow cytometry (FC) are two other, non-microscopical methods to measure spore size. CC is an electrometric instrument, which uses the Coulter principle. The change in resistance observed when a particle is pulled through an aperture is proportional to the volume of the particle. This change is relatively independent of shape of the particle and therefore, it is a fast and reliable method to determine spore volume, including those of non-spherical conidia (Valero-Jiménez, Debets, van Kan, Schoustra, Takken, Zwaan, & Koenraadt, 2014; van den Brule, Punt, Teertstra, Houbraken, Wösten, & Dijksterhuis, 2020). The forward scatter pulse area (FSC) in flow cytometry (FC) can be used as a proxy for cell size and has been used to indicate the size of germinating conidia of *Aspergillus niger* (Hayer, Stratford, & Archer, 2013, 2014). However, FSC intensities are not only influenced by the size of a cell or particle. The refraction index between the particle and the fluid, as well as the presence of pigment or other absorbing compounds can influence this parameter (Tzur, Moore, Jorgensen, Shapiro, & Kirschner, 2011). In addition, FSC values can differ by the FSC measurement design, which can vary per flow

cytometer. Therefore, FSC values are often used as a relative measure for size.

*Paecilomyces variotii* is a cosmopolitan food spoilage fungus that is capable of spoiling a broad range of products like canned fruits, non-carbonated sodas, margarine and rye bread (Pitt & Hocking, 2009). Previously, we have studied strain variation in *P. variotii* conidial heat resistance by screening 108 isolates. Three strains were used to quantify conidial heat resistance in terms of D-value and were further characterized by morphology, spore size distribution, compatible solute composition and their ability to grow in salt enriched medium. The conidia of strain DTO 217-A2 were found to be the most heat-resistant when compared to such spores of other fungal species (van den Brule, Punt, Teertstra, Houbraken, Wösten, & Dijksterhuis, 2020). *P. variotii* conidia are ellipsoid of shape with flattened apical edges and they can vary in size within and between cultures of different strains. Notably, the strain that produced the most heat-resistant conidia also produced conidia with the largest mean spore size as measured by CC, compared to two other strains (van den Brule, Punt, Teertstra, Houbraken, Wösten, & Dijksterhuis, 2020). The conidia of the heat-resistant strain also showed the widest spore size distribution with a bimodal character.

To investigate the influence of the heterogeneity in spore size on the heat resistance, it is important to measure spore size correctly. Therefore, our first objective in the present study was to compare various measurement techniques to elucidate their accuracy, advantages and disadvantages. LM, SEM and CC were used to compare the spherical equivalent diameter and CC and flow cytometry were used to study spore size distributions. Secondly, we studied the correlation between spore morphology as well as spore size distribution and heat resistance. Therefore, we quantified the conidial heat resistance for five heat sensitive and five heat resistant strains.

## 2. Methods and materials

### 2.1. Strain selection and growth conditions

Based on a previous published screening for conidial heat resistance, five heat-sensitive and heat-resistant *P. variotii* strains were selected (van den Brule, Punt, Teertstra, Houbraken, Wösten, & Dijksterhuis, 2020); Table 1). Cultures were inoculated on malt extract agar (MEA, Oxoid, Hampshire, UK) from glycerol stocks stored at -80° and incubated for 7 days at 25 °C. To avoid any glycerol background that could interfere with heat resistance, cultures were re-inoculated confluent on MEA. After another round of incubation for 7 days at 25 °C, spore suspensions were prepared as described previously (van den Brule, Punt, Teertstra, Houbraken, Wösten, & Dijksterhuis, 2020). Concentration of spore suspensions was determined by CC (see below) and set to a final concentration of  $2 \times 10^8$  conidia mL<sup>-1</sup> ACES buffer [10 mM N(2-acetamido)-2-aminoethanesulfonic acid, 0.02% Tween 80, pH 6.8]. Suspensions were stored on melting ice for maximum of 24 h

**Table 1**  
Strains used in this study.

DTO no.	CBS no.	Substrate	Location	Percentage survival after 10 min heat treatment <sup>1</sup>		Conidial heat resistance
				58 °C	59 °C	
DTO 032-I3	CBS 121585	HFCS after heat shock	USA	7.05	2.65	Sensitive
DTO 032-I4	CBS 121586	Spoiled bottle of sweetened tea	USA	6.75	ND	Sensitive
DTO 063-F5		Human; abscess	The Netherlands	3.25	0.5	Sensitive
DTO 166-G5		Pectin, heat treated	The Netherlands	>10	>10	Resistant
DTO 169-C6	CBS 145661	Indoor environment	USA	>10	>10	Resistant
DTO 169-E5	CBS 145662	Indoor environment	USA	1.25	0.05	Sensitive
DTO 195-F2	CBS 145663	Margarine	Belgium	>10	>10	Resistant
DTO 212-C5	CBS 145665	Vanilla	The Netherlands	5.8	0.3	Sensitive
DTO 217-A2	CBS 145666	Ice pop, heat treated	The Netherlands	>10	>10	Resistant
DTO 282-E5	CBS 145669	Margarine	Italy	>10	>10	Resistant

<sup>1</sup> van den Brule, Punt, Teertstra, Houbraken, Wösten, and Dijksterhuis (2020).

before further experiments.

## 2.2. Quantification of conidial heat-resistance

We quantified conidial heat-resistance as described (van den Brule, Punt, Teertstra, Houbraken, Wösten, & Dijksterhuis, 2020). To inactivate  $10^7$  conidia  $\text{mL}^{-1}$ , 1 mL  $2 \times 10^8$  conidia  $\text{mL}^{-1}$  was added to 19 mL pre-heated ACES buffer in 100 mL Erlenmeyer flasks at 60 °C and 120 rpm. After 2, 5, 15, 30 and 60 min, 1 mL samples were taken from the flasks and directly placed on ice to stop the inactivation process. All samples, including the untreated spore suspension, were further diluted to  $10^3$  conidia  $\text{mL}^{-1}$ . A volume of 100  $\mu\text{L}$  of each dilution was spread plated on a 9 cm Petri dish. Plates that showed between 1 and 150 colonies after three days of incubation at 25 °C were used to determine the log colony forming units (CFU)  $\text{mL}^{-1}$ . Inactivation was described by a linear regression curve of the logCFU  $\text{mL}^{-1}$  against the inactivation time. The  $D_{60}$ -values, which express the decimal reduction time, were determined by  $\frac{-1}{\text{slope}}$  of the inactivation curve. All experiments were performed using biological triplicates.

## 2.3. Microscopy

For LM, approximately 10  $\mu\text{L}$  of spore suspension was mixed with lactic acid containing aniline blue (0.05% (w/v) methyl blue in 90% (S)-lactic acid) on a glass slide. Images were captured by a Zeiss Axioskop 2 Plus Light microscope equipped with a Nikon DS-Fi1 camera and 63 $\times$  oil objective to achieve a 630 $\times$  magnification. The microscope was calibrated using a scale bar at the same magnification.

To prepare samples for cryo-SEM, a small piece of MEA of approximately 5  $\times$  5 mm in size was glued in a copper cup by frozen tissue medium (KP-Cryoblock, Klinipath, Duiven, The Netherlands). Approximately 1  $\mu\text{L}$  of conidia suspension was transferred to polycarbonate filter paper (GE Water & Process Technologies). The filter paper with conidia on top was then transferred to the surface of the agar block prepared previously. Together with the agar block, the sample was snap-frozen in liquid nitrogen slush. Ice formed on sample surface was removed by sublimation at  $-85$  °C. The frozen specimen was sputter-coated using a gold target before imaging using a JEOL 5600LV microscope (Tokyo, Japan) with an Oxford CT1500 Cryostation, and viewed using an acceleration voltage of 5 kV. The scan 4 mode was used for image acquisition.

Images of a hundred conidia per strain were selected randomly from both light- and electron microscopy micrographs for spore size measurement. The images were analyzed by ImageJ software (<https://imagej.nih.gov/ij/index.html>). An ellipse was fitted around the selected conidium and the major and minor axis, as well as the area and perimeter were determined. Spore size is expressed by the diameter of the spherical equivalent and was calculated by  $\varnothing = 2 * \sqrt[3]{\frac{\text{major}}{2} * (\frac{\text{minor}}{2})^2}$ . The spore shape parameters aspect ratio (AR), circularity (C) and roundness (R) were calculated by  $AR = \frac{\text{major}}{\text{minor}}$ ,  $C = \frac{4\pi * \text{area}}{\text{perimeter}^2}$  and  $R = \frac{4 * \text{area}}{\pi * \text{major}^2}$ , respectively.

## 2.4. Coulter counter and flow cytometry

Before the concentrations were set, spore suspensions were diluted  $2 \times 10^3$  times in ISOTON II diluent (Beckman Coulter, Fichtenhain, Germany) prior to CC analysis. A Beckman Coulter Counter Multisizer 3 equipped with a 70- $\mu\text{m}$  aperture tube was used to determine the concentration of the original spore stocks. Pulse data of a thousand data points were randomly selected from the CC analysis to study spore size distribution. CC was calibrated using latex beads with a diameter of 5, 10 and 20  $\mu\text{m}$  (Beckman Coulter, Brea, CA, USA). The following parameters were determined using the CC data. The P90/P10 ratio was calculated by dividing the ninth decile by the first decile. The span was calculated by  $\frac{P90 - P10}{P50}$ , where P50 represents the median. Skewness was

determined by  $b1 = \frac{m_3}{s^3} = \left(\frac{n-1}{n}\right)^{3/2} \frac{m_3}{m_2^{3/2}}$  where  $m_r = \frac{1}{n} \sum (x_i - \mu)^r$  and  $s^2 = \frac{1}{n-1} \sum (x_i - \mu)^2$  (Joanes & Gill, 1998).

For FC, a concentration of  $2 \times 10^7$  conidia  $\text{mL}^{-1}$  was analyzed using a FACSVerse™ (Becton Dickinson, Franklin Lakes, NJ). Like the coulter counter data, a thousand data points of FSC pulse area were randomly selected to analyze spore size distributions.

## 2.5. Statistics

QQ-plots of LM, SEM and CC data revealed that not all data was normally distributed. Therefore, the Friedman's test ( $\alpha < 0.05$ ) was used to describe differences in spore size between strains and methods. Boxplot elements indicate the median, the hinges representing the 25th and 75th percentiles, the upper whisker representing  $1.5 * \text{Inter Quartile Range (IQR)}$  from the hinge and the lower whisker extends to the lowest value, at most  $1.5 * \text{IQR}$ . Data beyond the range of the whiskers are considered outliers. Spore size distributions of the CC and FC data were analyzed using the Mixtools package in R (Benaglia, Chauveau, Hunter, & Young, 2009). Data of both measurement methods were analyzed by means of a two-component mixture model. The boot.comp function with 1000 parametric bootstraps was used to test significance  $P(k > 1) < 0.05$ , where k is the number of components. In each distribution, two populations were computed using Expectation Maximization (EM) algorithm using the normalmixEM function. Standard errors of the mean ( $\mu$ ), standard deviation ( $\sigma$ ) and weight related to the total population ( $\lambda$ ) were determined by the boot.se function using 1000 parametric bootstraps.

## 3. Results

### 3.1. Selection of *P. variotii* strains and quantification of conidial heat resistance

Ten strains of *P. variotii* were selected from the Westerdijk Fungal Biodiversity Institute collection (Table 1). Seven strains were originating from food products, two from the indoor environment and one from a human patient. The strains were selected based on their results of a screening for conidial heat resistance (van den Brule, Punt, Teertstra, Houbraken, Wösten, & Dijksterhuis, 2020). The conidial heat resistance of the strains was quantified by studying inactivation kinetics at 60 °C (Table 2, Fig. 1). For 9 out of 10 strains the inactivation kinetics showed a highly linear character ( $R^2 < 0.90$ ). Only DTO 169-E5 showed a lower value at  $R^2 = 0.81$ . From the inactivation curve, the decimal reduction time ( $D_{60}$ -value) was calculated, which represents the time to cause 1 log reduction at 60 °C. DTO 195-F2 produced the most heat-resistant conidia with a  $D_{60}$ -value of  $27.6 \pm 3.12$  min, whereas the conidia of DTO 063-F5 were the most heat sensitive with a  $D_{60}$ -value of  $3.5 \pm 0.20$  min. All heat-sensitive strains showed a  $D_{60}$ -value  $\leq 6$  min, while the five heat-resistant strains had a  $D_{60}$ -value  $> 9$  min.

**Table 2**

Conidial heat resistance expressed by D-value. Average value  $\pm$  SD is shown of three biological replicates.

Strain	$D_{60}$ -value (min)	$R^2$
DTO 032-I3	$6.0 \pm 0.70$	0.979
DTO 032-I4	$4.9 \pm 1.73$	0.906
DTO 063-F5	$3.5 \pm 0.20$	0.961
DTO 166-G5	$11.9 \pm 1.28$	0.983
DTO 169-C6	$9.4 \pm 0.50$	0.992
DTO 169-E5	$5.0 \pm 1.97$	0.805
DTO 195-F2	$27.6 \pm 3.12$	0.953
DTO 212-C5	$3.6 \pm 0.19$	0.963
DTO 217-A2	$20.1 \pm 4.02$	0.924
DTO 282-E5	$14.2 \pm 2.20$	0.956

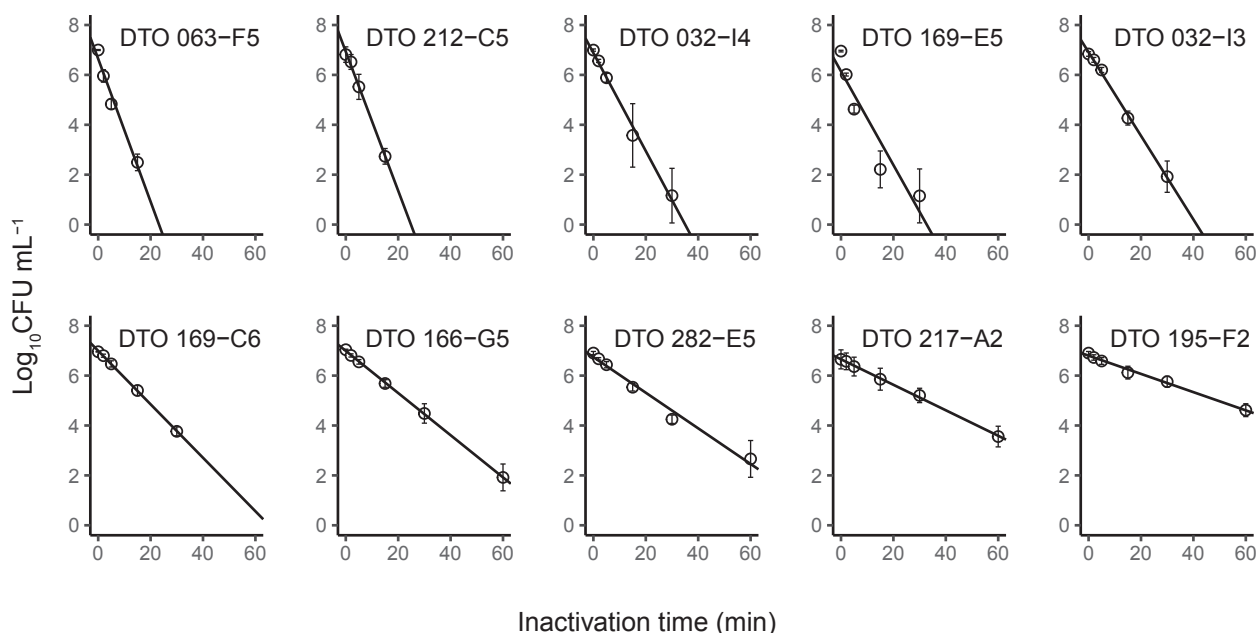


**Fig. 1.** Heat inactivation curves of conidia originating from 10 *P. variotii* strains, ordered from most heat sensitive (DTO 063-F5) to most heat resistant (DTO 195-F2). A linear regression was fitted to the mean data points of three independent measurements. Error bars indicate standard deviations of biological triplicates.

### 3.2. Comparison of light microscopy, scanning electron microscopy, and coulter counter to measure spore size

The size of the ellipsoid shaped conidia of *P. variotii* was expressed as one integer: the so-called Heywood diameter, which designates the spherical equivalent. In case of the two-dimensional microscopic pictures, this parameter was estimated by fitting an ellipse as accurately as possible around the spores (Fig. 2A–D). From this ellipse, the major and minor axis were determined and used to calculate the spherical equivalent diameter. The CC software converts the Heywood diameter based on calibration with latex beads of a defined size. Data of 100 randomly selected spores of the ten *P. variotii* strains were obtained using LM, SEM and CC (Fig. 2E). QQ-plots revealed that not all spore size distributions were normally distributed (data not shown). Therefore, we used thenon-parametric Friedman's test to test for significant differences between strains and methods. Significant differences in spore size were found ( $\chi^2 = 19.873$ ,  $df = 9$ ,  $P = 0.019$ ) when spore size between strains was compared, while we did not find significant differences between the measuring methods ( $\chi^2 = 0.6$ ,  $df = 2$ ,  $P = 0.741$ ).

### 3.3. Comparison of coulter counter and flow cytometry to study spore size distributions

A thousand data points of CC and FC were randomly selected to study spore size distributions. To test if the distributions could be described by more than one component, we tested  $P(k > 1)$  using the boot.comp function with 1000 bootstraps of the mixtools package in R (Benaglia, Chauveau, Hunter, & Young, 2009). In all cases we found  $P(k > 1) < 0.001$ , meaning that the spore size distribution can be described by two or more normal distributions. Two normal distributions were computed for each spore size distribution using EM algorithm (Table 3). In this analysis, we modelled two populations of different spore size within one spore size distribution. The small size spore population contains a mean spore size of  $\mu_1$  with a standard deviation of  $\sigma_1$ , whereas the large size spore population is expressed by  $\mu_2$  and  $\sigma_2$ . The proportion of each population is expressed by weight parameter  $\lambda_1$  and  $\lambda_2$  for the population of small spore size and large spore size, respectively. To test if the means of the two populations were statistically

significant different, a 99% confidence interval was calculated. All strains showed no overlap in the confidence interval of the two computed populations, indicating that  $\mu_1$  and  $\mu_2$  are significantly different in all cases.

Spore size distributions as measured with FC and CC showed similar patterns for seven out of ten strains (Fig. 3, Table 3). The conidia population of strain DTO 217-A2 was predominated by  $\lambda_2$  of 0.80 and 0.75 in the CC and FC results, respectively. In addition, clear predominance of  $\lambda_2$  is observed in DTO 166-G5. DTO 032-I3 showed highest predominance of the small spore size population with  $\lambda_1$  with 0.72 and 0.78 in the CC and FC results, respectively. Predominance of the  $\lambda_1$  was seen in the case of strains DTO 169-C6, DTO 063-F5 (only CC data) and DTO 169-E5 and 032-I4 (only FC data). Four strains showed about equal distribution of  $\lambda_1$  (0.42–0.54) and  $\lambda_2$  (0.46–0.58). Three strains showed difference of population predominance of large size conidia ( $\lambda_2$ , strain DTO 063-F5) between CC ( $\lambda_2 = 0.27$ ) and FC ( $\lambda_2 = 0.44$ ). The opposite was found for DTO 032-I4 and DTO 169-E5, showing smaller weight for the population large spores when measured by FC ( $\lambda_2 = 0.18$  and 0.28, respectively) than CC ( $\lambda_2 = 0.45$  and 0.44, respectively). Together, these results revealed differences in spore size distribution among *P. variotii* strains.

### 3.4. Correlations of conidial heat resistance and mean spore size, spore shape, as well as size distributions

In a previous study, it was noted that heat-resistant strain DTO 217-A2 produced on average larger conidia than two heat-sensitive strains (van den Brule, Punt, Teertstra, Houbraken, Wösten, & Dijksterhuis, 2020). Furthermore, the  $\lambda_2$  of this strain was larger compared to the other two strains. Pearson correlation analyses were used to test whether spore shape parameters correlate with heat resistance (Table 4, Fig. 4). The tested shape parameters included aspect ratio (AR), roundness (R) and circularity (C) and were based on the measurements of 100 conidia on LM micrographs. In addition, as determined by a thousand data points obtained by CC, the mean spore size and the distribution parameters p90/p10 ratio, span, skewness and  $\lambda_2$  were compared with the log  $D_{60}$ -value. The mean spore size was significantly positively correlated with heat resistance, suggesting that resistant strains produce larger spores than heat-sensitive strains. The shape

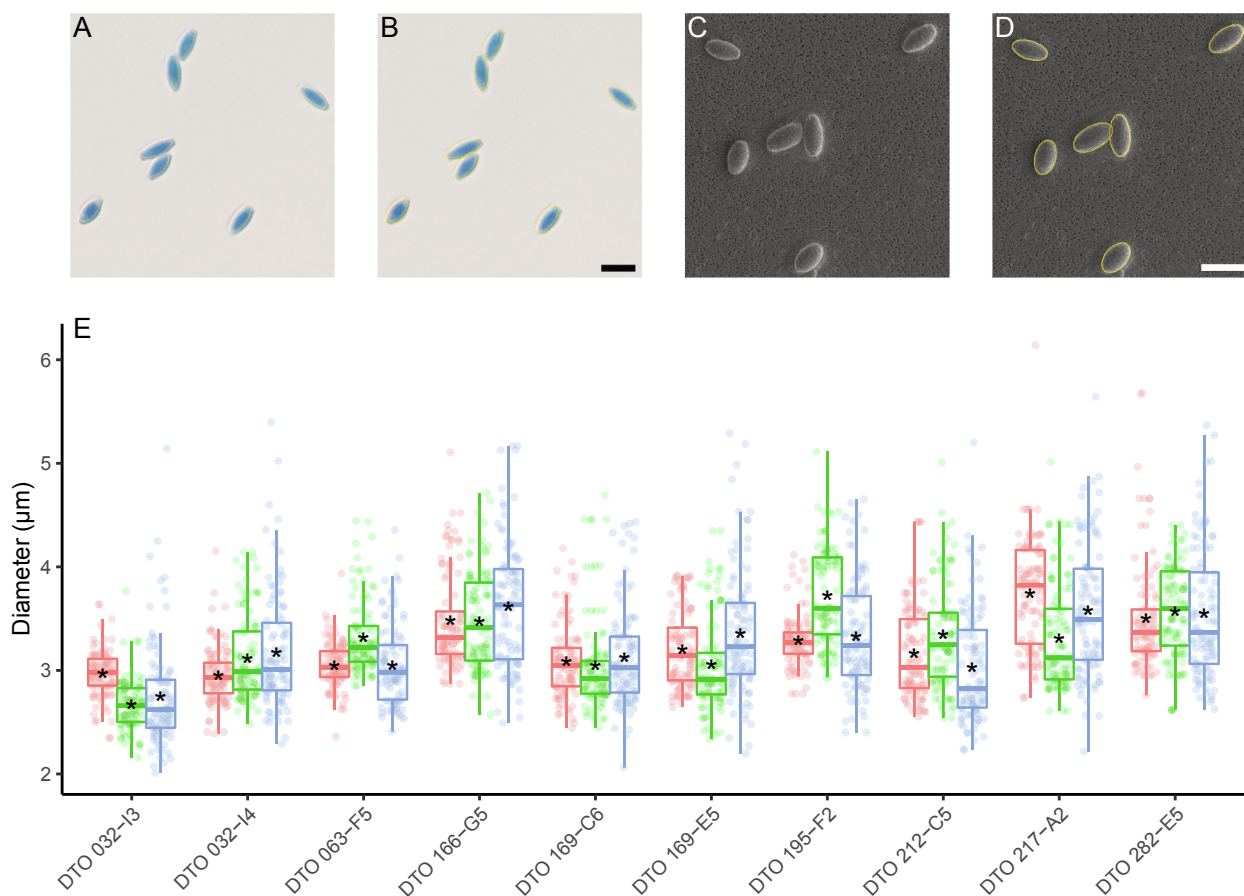


**Fig. 2.** Conidia size measurements of *P. variotii* strains. Pictures of *P. variotii* DTO 032-I3 conidia made by light microscopy (A, B) or scanning electron microscopy (C, D). To measure spore size, a yellow ellipse was fitted around the particles (B, D). Scale bars indicate 10 µm. (E) Comparison of spore diameter distributions of 10 data points obtained by LM (red), SEM (green) and CC (blue) for 10 *P. variotii* strains. The asterisk indicates the mean spore size. (For interpretation of the references to colour in this figure legend, the reader is referred to the web version of this article.)

**Table 3**

Two populations of spore size as modelled by computation of the measurements by means of Coulter Counter (CC) and Flow Cytometry (FC). The mean and standard deviation are expressed by  $\mu$  and  $\sigma$ , respectively. The weight each population compared to the total population is expressed by  $\lambda$ . Standard errors are included to each value of the mixture models.

Strain	Method	Population 1			Population 2		
		$\mu_1^a$	$\sigma_1^a$	$\lambda_1^b$	$\mu_2^a$	$\sigma_2^a$	$\lambda_2^b$
DTO 032-I3	CC	2.59 ± 0.011	0.23 ± 0.011	0.72 ± 0.036	3.33 ± 0.092	0.57 ± 0.045	0.28 ± 0.036
	FC	35601 ± 484	12228 ± 421	0.78 ± 0.019	100875 ± 5018	47650 ± 2915	0.22 ± 0.019
DTO 032-I4	CC	2.88 ± 0.015	0.24 ± 0.016	0.55 ± 0.045	3.5 ± 0.068	0.62 ± 0.029	0.45 ± 0.045
	FC	63844 ± 538	13046 ± 515	0.82 ± 0.028	103589 ± 6402	36007 ± 3259	0.18 ± 0.028
DTO 063-F5	CC	2.94 ± 0.011	0.24 ± 0.01	0.73 ± 0.029	3.59 ± 0.076	0.71 ± 0.036	0.27 ± 0.029
	FC	81358 ± 667	11525 ± 640	0.56 ± 0.031	92415 ± 2412	47697 ± 2008	0.44 ± 0.031
DTO 166-G5	CC	3.09 ± 0.015	0.17 ± 0.015	0.33 ± 0.031	3.71 ± 0.034	0.6 ± 0.018	0.67 ± 0.031
	FC	97702 ± 905	12158 ± 880	0.41 ± 0.032	136701 ± 2587	43699 ± 1327	0.59 ± 0.032
DTO 169-C6	CC	2.91 ± 0.019	0.29 ± 0.018	0.64 ± 0.062	3.6 ± 0.13	0.63 ± 0.055	0.36 ± 0.062
	FC	71419 ± 988	18005 ± 984	0.59 ± 0.036	136234 ± 5587	47599 ± 2904	0.41 ± 0.036
DTO 169-E5	CC	2.97 ± 0.017	0.27 ± 0.018	0.56 ± 0.05	3.73 ± 0.09	0.63 ± 0.04	0.44 ± 0.05
	FC	39821 ± 503	11781 ± 440	0.72 ± 0.021	99189 ± 4275	43807 ± 2393	0.28 ± 0.021
DTO 195-F2	CC	2.99 ± 0.019	0.24 ± 0.017	0.52 ± 0.058	3.68 ± 0.079	0.52 ± 0.037	0.48 ± 0.058
	FC	93725 ± 979	15692 ± 1038	0.58 ± 0.045	124187 ± 3668	40132 ± 1692	0.42 ± 0.045
DTO 212-C5	CC	2.69 ± 0.016	0.24 ± 0.017	0.52 ± 0.047	3.38 ± 0.072	0.59 ± 0.033	0.48 ± 0.047
	FC	59889 ± 618	12122 ± 600	0.56 ± 0.025	122312 ± 3414	45483 ± 1966	0.44 ± 0.025
DTO 217-A2	CC	2.95 ± 0.023	0.17 ± 0.025	0.2 ± 0.035	3.69 ± 0.035	0.56 ± 0.018	0.8 ± 0.035
	FC	91821 ± 1037	10064 ± 978	0.25 ± 0.026	143597 ± 2053	39486 ± 1198	0.75 ± 0.026
DTO 282-E5	CC	3.17 ± 0.019	0.27 ± 0.019	0.52 ± 0.053	3.92 ± 0.086	0.62 ± 0.039	0.48 ± 0.053
	FC	97258 ± 1479	18597 ± 1400	0.46 ± 0.049	159014 ± 5151	42850 ± 2640	0.54 ± 0.049

a. FC  $\mu$  and  $\sigma$  values are expressed by Forward scatter (arbitrary units) and CC values expressed the spherical equivalent diameter (µm).

b. The sum of  $\lambda_1$  and  $\lambda_2$  equals 1.

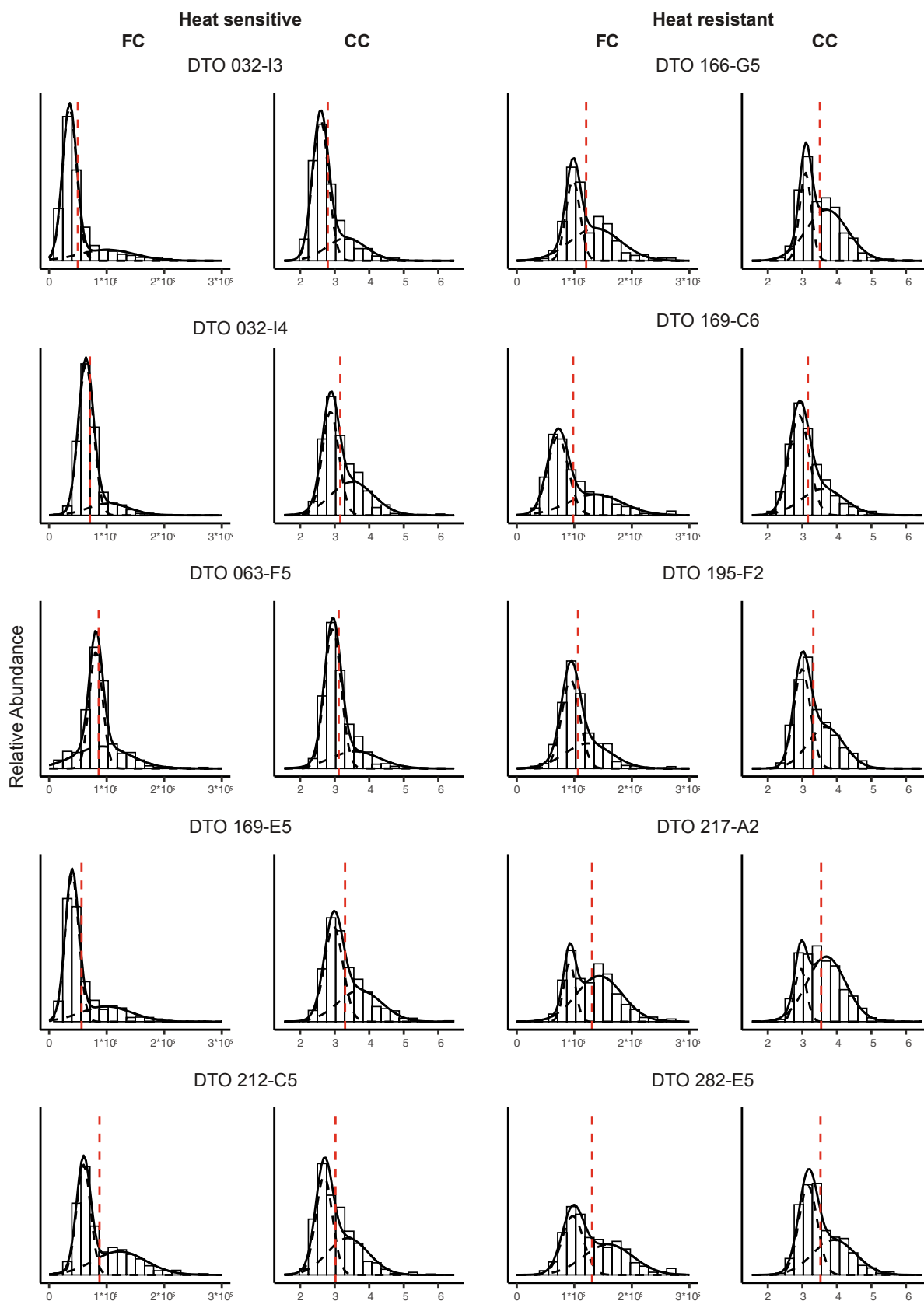


**Fig. 3.** Spore size distributions of 10 *P. variotii* strains as measured by FC and CC. The total surface of the histogram bars equals 1. All distributions were described by two populations (black dashed lines) which were computed using EM algorithm. In addition, the sum of the two populations (black solid line) and the mean spore size values (red dashed line) is shown in the plots. FC values are expressed by FSC and CC values expressed the spherical equivalent diameter. (For interpretation of the references to colour in this figure legend, the reader is referred to the web version of this article.)

**Table 4**  
Pearson correlations of conidial heat resistance ( $\log_{10}D$ -value) with various spore size distribution and spore shape parameters.

Variable	Correlation coefficient (r)	P-value	Significance ( $p < 0.05$ )
<i>Spore shape parameters</i>			
Mean spore size	0.65	0.044	*
AR*	-0.67	0.034	*
C*	0.67	0.033	*
R*	0.68	0.030	*
<i>Spore distribution parameters</i>			
$\lambda_2$	0.57	0.083	
p90/p10	0.28	0.433	
sk*	-0.64	0.044	*
span	0.20	0.583	

\*Abbreviations: AR, Aspect Ratio; C, circularity; R, roundness; sk, skewness.

parameters aspect ratio, circularity and roundness also correlated significantly with heat resistance. For all three parameters, a perfect circle has a value of 1. Since conidia of heat resistant strains tend to have values closer to 1 than heat sensitive strains, these results suggest that the ellipsoidal spores of heat-resistant strains are more spherical in shape than those of sensitive strains that are more elongated. The values of the spore size distribution parameters p90/p10 and span, that both address the width of the spore size distribution, did not correlate with heat resistance. The weight of the population large conidia ( $\lambda_2$ ) also did not correlate with heat resistance. At last, the spore size distribution parameters skewness showed a significant negative correlation with heat resistance, implying that the sensitive strains produce relatively more outliers in respect to conidia size than resistant strains.

#### 4. Discussion

Heterogeneity in heat resistance, size and shape of conidia of the food-spoiling fungus *P. variotii* was determined. Five heat-sensitive and five heat-resistant strains were selected based on a previous screening (van den Brule, Punt, Teertstra, Houbraken, Wösten, & Dijksterhuis,

2020). Conidia of the five heat-sensitive strains showed a  $D_{60}$ -value of 3.5–6.0 min, while  $D_{60}$ -values of 9.4–27.6 min were observed for the resistant strains. Strain DTO 195-F2 produced most heat-resistant conidia and its spores are more resistant than those of *P. variotii* DTO 217-A2 that were so far the most heat-resistant conidia produced by fungi. Thus, DTO 195-F2 produces the most heat-resistant conidia ever reported. Also of interest, we here show a correlation between heat resistance and spore size and shape.

Conidia size was determined using LM, SEM, CC and FC. The latter did not show a linear correlation with cell size when forward scatter was used but can be used to study the cell size distribution. Data obtained with LM, SEM and CC all confirmed differences in conidia size between the strains. For all three methods, we used the Heywood diameter as one integer to describe the ellipsoid conidia size. Spore size varies among the tested strains ranging from an average of 2.7  $\mu\text{m}$  for DTO 032-I3 to 3.6  $\mu\text{m}$  for DTO 166-G5. These differences in spore size imply a 2.4 fold difference in spore volume of the conidia of the strains producing the smallest and largest conidia.

Spore sizes measure with LM, SEM and CC were not statistically different. LM is based on transmitted light; SEM uses a scanning electron beam and CC measures the impedance of a particle in an aperture. These three methods each have their own sources of variation illustrated by the halo around objects in the case of LM and the drift of a sample during SEM. In another study, larger sizes were found when measuring *Penicillium* conidia by (environmental) SEM compared to LM, because the higher magnifications revealed the ornamentation of the spores better (Reponen, Grinshpun, Conwell, Wiest, & Anderson, 2001). In the case of the smooth walled *P. variotii* conidia this is not a problem, but it should be taken into account when measuring ornamented spores by any microscopy technique. Of interest, CC showed a larger standard deviation in spore size than the microscope techniques for all 10 strains. This may be caused by the fact that CC may also measure hyphal fragments or phialides occasionally. In summary, our data showed that as long as the machinery is calibrated well, it seems not to matter which technique is used to determine spore size. The advantages and disadvantages of each technique are summarized in Table 5.

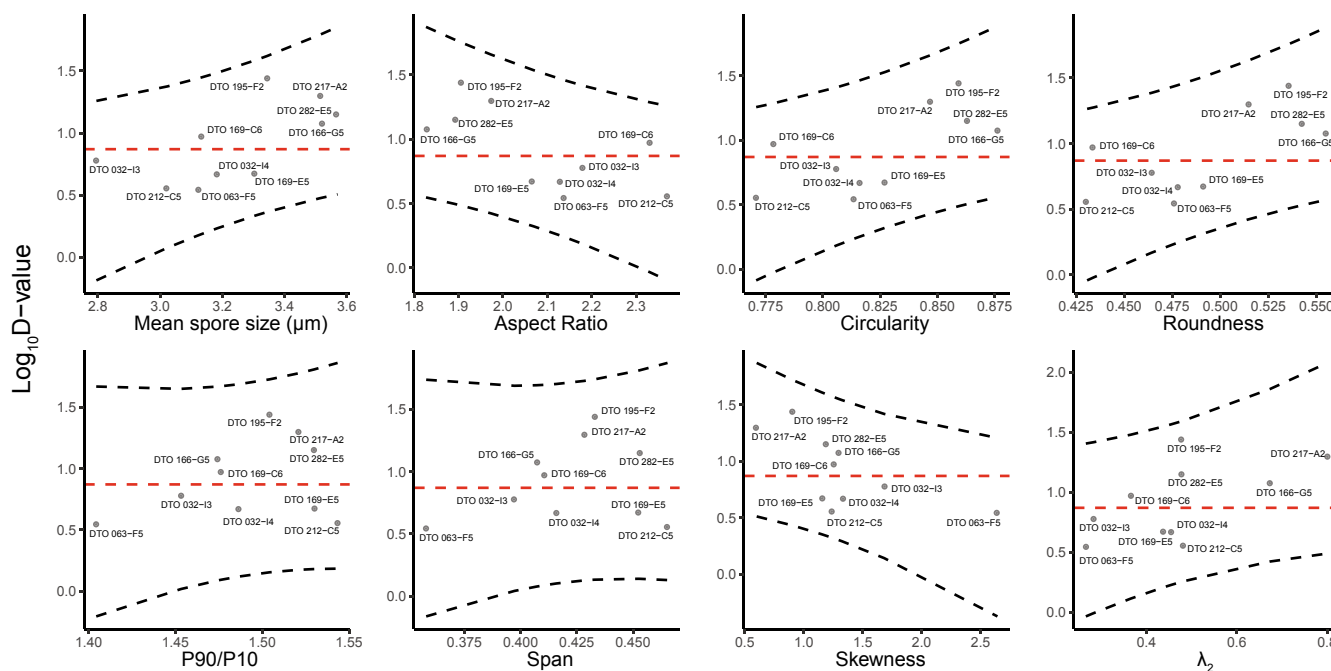


**Fig. 4.** Pearson correlations of the  $\log_{10}D$ -value and various spore size and spore shape parameters. The black dashed lines indicate the 95% prediction interval and the red dashed line indicates the boundary between heat resistant strains and heat sensitive strains. (For interpretation of the references to colour in this figure legend, the reader is referred to the web version of this article.)

**Table 5**

Advantages and disadvantages of each technique discussed in this study to measure spore size, spore shape and spore size distribution.

Technique	Advantages	Disadvantages
Light Microscopy	<ul style="list-style-type: none"> <li>Available to every lab with a light microscope</li> <li>Shape can be studied</li> </ul>	<ul style="list-style-type: none"> <li>Spore selection could lead to a bias in heterogeneity</li> <li>Halo formation</li> </ul>
Scanning Electron Microscopy	<ul style="list-style-type: none"> <li>No halo formation</li> <li>Shape can be studied</li> </ul>	<ul style="list-style-type: none"> <li>Spore selection could lead to a bias in heterogeneity</li> <li>Laborious</li> </ul>
Coulter Counter	<ul style="list-style-type: none"> <li>Fast measurements</li> <li>Measures particles regardless of shape</li> </ul>	<ul style="list-style-type: none"> <li>Spore complexes and other particles are not identified</li> <li>Shape cannot be studied</li> </ul>
Flow cytometry	<ul style="list-style-type: none"> <li>Fast measurements</li> </ul>	<ul style="list-style-type: none"> <li>FSC does not correlate with spherical equivalent diameter</li> <li>Orientation of non-spherical spores may influence FSC values.</li> <li>Shape cannot be studied</li> </ul>

Spore size of *P. variotii* correlated with heat resistance thus suggesting a causal relation. This hypothesis is in agreement with results of ascospores of the closely related fungal species *Talaromyces flavus* and *Talaromyces macrosporus* (Frisvad, Filtenborg, Samson, & Stolk, 1990). The size of the ellipsoidal ascospores is  $4\text{--}5.5 \times 3\text{--}3.5 \mu\text{m}$  for *T. flavus* and  $5\text{--}6.5 \times 4.5\text{--}5.5 \mu\text{m}$  for *T. macrosporus* and the ascospores of the latter are much more heat-resistant (Beuchat, 1988; Dijksterhuis, 2019; Yilmaz, Visagie, Houbraken, Frisvad, & Samson, 2014). The spores of both species have a similar composition of compatible solutes and have a high concentration trehalose (Wyatt, van Leeuwen, Golovina, Hoekstra, Kuenstner, Palumbo, & Dijksterhuis, 2015). Similarly, the large *Aspergillus spinosus* ascospores have a higher heat resistance than the smaller *A. fischeri* (unpublished data). This could be even hold for other stresses; larger sporangiospores of *Mucor circinelloides* are more virulent and survive and germinate inside macrophages, while smaller spores do not (Li, Cervantes, Springer, Boekhout, Ruiz-Vazquez, Torres-Martinez, & Lee, 2011).

An advantage in determining spore size using a microscope is that it gives extra spore shape parameters. The major and minor axis determined by the fitted ellipses around the spores were used to calculate the aspect ratio, circularity and roundness of the spores. Surprisingly, all these parameters correlated with heat resistance, indicating that conidia formed by heat-resistant strains have a higher sphericity than conidia formed by sensitive strains. Similar as small spore size, a low sphericity results in a larger surface-area-to-volume ratio and might therefore cause a higher susceptible to heat stress. We assume that the small spore sizes have a negligible effect on heat transfer into the spores with different size. Yet, the surface area of the plasma membrane would explain the differences in heat resistance. Thus, future studies should assess whether the primary effect of conidial killing acts on the plasma membrane.

It has been described before that differences occur in spore size distributions among three *P. variotii* strains (van den Brule, Punt, Teertstra, Houbraken, Wösten, & Dijksterhuis, 2020). In this study, FC and CC analysis of seven additional strains confirmed that the conidial spore size distribution is clearly different among strains. Interestingly, the skewness of the distribution was significantly negatively correlated with heat resistance. This indicates that strains producing heat-sensitive spores are likely to produce more outliers in respect to conidia size than heat-resistant strains. Notably, all spore size distributions were slightly positively skewed. It should be noted that correlation coefficients are relatively low, indicating that exceptions might occur. This is illustrated by the heat-resistant conidia of DTO 169-C6 that show a low mean spore size and similar shape as characterized by the other heat-sensitive strains. Summarized, conidial size, shape and the skewness of the cell size distribution of *P. variotii* strains could be used as indicators for heat resistance.

With this study, we analysed spore size distributions of 10 *P. variotii* strains into detail. The diversity found in all parameters in this study, contributes to a better understanding in spore heterogeneity of fungal species. Microbial heterogeneity is an important factor in predictive food mycology, since spoilage can occur if only one spore is able to

germinate. In the end, the strongest spore will define if spoilage can occur.

### CRedit authorship contribution statement

**Tom van den Brule:** Conceptualization, Methodology, Data curation, Writing - original draft. **Cheuk Lam Sherlin Lee:** Methodology, Data curation. **Jos Houbraken:** Supervision. **Pieter Jan Haas:** Resources. **Han Wösten:** Supervision, Writing - review & editing. **Jan Dijksterhuis:** Conceptualization, Supervision, Writing - review & editing.

### Acknowledgements

We would like to thank all people involved in the TiFN spores project for their consult in this research. In addition, we would like to thank Martin Meijer and Bart Kraak for their support in the lab and Basten Snoek for his help on the statistical analyses.

### References

- Aldrich, H. C., & Todd, W. J. (1986). *Ultrastructure Techniques for Microorganisms*. New York: Plenum Press.
- Andersen, B., Frisvad, J. C., Søndergaard, I., Rasmussen, I. S., & Larsen, L. S. (2011). Associations between Fungal Species and Water-Damaged Building Materials. *Applied and Environment Microbiology*, 77(12), 4180–4188. <https://doi.org/10.1128/aem.02513-10>.
- Benaglia, T., Chauveau, D., Hunter, D., & Young, D. (2009). mixtools: An R package for analyzing finite mixture models. *Journal of Statistical Software*, 32(6), 1–29.
- Beuchat, L. R. (1988). Influence of organic acids on heat resistance characteristics of *Talaromyces flavus* ascospores. *International Journal of Food Microbiology*, 6(2), 97–105. [https://doi.org/10.1016/0168-1605\(88\)90046-3](https://doi.org/10.1016/0168-1605(88)90046-3).
- Chen, A. J., Frisvad, J. C., Sun, B. D., Varga, J., Kocsubé, S., Dijksterhuis, J., ... Samson, R. A. (2016). *Aspergillus* section *Nidulantes* (formerly *Emericella*): Polyphasic taxonomy, chemistry and biology. *Studies in Mycology*, 84, 1–118. <https://doi.org/10.1016/j.simyco.2016.10.001>.
- Dijksterhuis, J. (2019). Fungal spores: Highly variable and stress-resistant vehicles for distribution and spoilage. *Food Microbiology*, 81, 2–11. <https://doi.org/10.1016/j.fm.2018.11.006>.
- dos Santos, J. L. P., Samapundo, S., Biyikli, A., Van Impe, J., Akkermans, S., Höfte, M., ... Devlieghere, F. (2018). Occurrence, distribution and contamination levels of heat-resistant moulds throughout the processing of pasteurized high-acid fruit products. *International Journal of Food Microbiology*, 281, 72–81. <https://doi.org/10.1016/j.ijfoodmicro.2018.05.019>.
- Frisvad, J. C., Filtenborg, O., Samson, R. A., & Stolk, A. C. (1990). Chemotaxonomy of the genus *Talaromyces*. *Antonie van Leeuwenhoek*, 57(3), 179–189. <https://doi.org/10.1007/BF00403953>.
- Geoghegan, I. A., Stratford, M., Bromley, M., Archer, D. B., & Avery, S. V. (2020). Weak Acid Resistance A (WarA), a Novel Transcription Factor Required for Regulation of Weak-Acid Resistance and Spore-Spore Heterogeneity in *Aspergillus niger*. *mSphere*, 5(1), e00685–00619. <https://doi.org/10.1128/mSphere.00685-19>.
- Hayer, K., Stratford, M., & Archer, D. B. (2013). Structural features of sugars that trigger or support conidial germination in the filamentous fungus *Aspergillus niger*. *Applied and Environment Microbiology*, 79(22), 6924–6931. <https://doi.org/10.1128/AEM.02061-13>.
- Hayer, K., Stratford, M., & Archer, D. B. (2014). Germination of *Aspergillus niger* conidia is triggered by nitrogen compounds related to L-amino acids. *Applied and Environment Microbiology*, 80(19), 6046–6053. <https://doi.org/10.1128/AEM.01078-14>.
- Hitchins, A. D., Kahn, A. J., & Slepecky, R. A. (1968). Interference contrast and phase contrast microscopy of sporulation and germination of *Bacillus megaterium*. *Journal of Bacteriology*, 96(5), 1811–1817.
- Joanes, D. N., & Gill, C. A. (1998). Comparing measures of sample skewness and kurtosis.



- Journal of the royal statistical society. Series D (The Statistician)*, 47(1), 183–189. <https://doi.org/10.1111/1467-9884.00122>.
- Leyva Salas, M., Mounier, J., Valence, F., Coton, M., Thierry, A., & Coton, E. (2017). Antifungal microbial agents for food biopreservation—A Review. *Microorganisms*, 5(3), 37.
- Li, C. H., Cervantes, M., Springer, D. J., Boekhout, T., Ruiz-Vazquez, R. M., Torres-Martinez, S. R., ... Lee, S. C. (2011). Sporangiospore Size Dimorphism Is Linked to Virulence of *Mucor circinelloides*. *PLoS Pathogens*, 7(6), Article e1002086. <https://doi.org/10.1371/journal.ppat.1002086>.
- Pitt, J. I., & Hocking, A. D. (2009). *Fungi and food spoilage* (3th ed.). New York: Springer.
- Punt, M., van den Brule, T., Teertstra, W. R., Dijksterhuis, J., den Besten, H. M. W., Ohm, R. A., & Wösten, H. A. B. (2020). Impact of maturation and growth temperature on cell-size distribution, heat-resistance, compatible solute composition and transcription profiles of *Penicillium roqueforti* conidia. *Food Research International*, 136, Article 109287. <https://doi.org/10.1016/j.foodres.2020.109287>.
- Reponen, T., Grinshpun, S. A., Conwell, K. L., Wiest, J., & Anderson, M. (2001). Aerodynamic versus physical size of spores: Measurement and implication for respiratory deposition. *Grana*, 40(3), 119–125. <https://doi.org/10.1080/00173130152625851>.
- Samson, R. A., Houbbraken, J., Thrane, U., Frisvad, J. C., & Andersen, B. (2019). *Food and indoor fungi. Westerdijk Laboratory Manual Series No. 2* (2nd ed.). Utrecht: Westerdijk Fungal Biodiversity Institute.
- Segers, F. J. J., van Laarhoven, K. A., Huinink, H. P., Adan, O. C. G., Wösten, H. A. B., & Dijksterhuis, J. (2016). The Indoor Fungus *Cladosporium halotolerans* Survives Humidity Dynamics Markedly Better than *Aspergillus niger* and *Penicillium rubens* despite Less Growth at Lowered Steady-State Water Activity. *Applied and Environmental Microbiology*, 82(17), 5089. <https://doi.org/10.1128/AEM.00510-16>.
- Staugaard, P., Samson, R. A., & Van der Horst, M. I. (1990). Variation in *Penicillium* and *Aspergillus* conidia in relation to preparatory techniques for scanning electron and light microscopy. In R. A. Samson, & J. I. Pitt (Vol. Eds.), *Modern Concepts in Penicillium and Aspergillus Classification: Vol. 185*, (pp. 39–48). Boston, MA: Springer.
- Tzur, A., Moore, J. K., Jorgensen, P., Shapiro, H. M., & Kirschner, M. W. (2011). Optimizing Optical Flow Cytometry for Cell Volume-Based Sorting and Analysis. *PLoS ONE*, 6(1), Article e16053. <https://doi.org/10.1371/journal.pone.0016053>.
- Ulevičius, V., Pečiulytė, D., Lugauskas, A., & Andriejauskienė, J. (2004). Field study on changes in viability of airborne fungal propagules exposed to UV radiation. *Environmental Toxicology*, 19(4), 437–441. <https://doi.org/10.1002/tox.20044>.
- Valero-Jiménez, C. A., Debets, A. J. M., van Kan, J. A. L., Schoustra, S. E., Takken, W., Zwaan, B. J., & Koenraadt, C. J. M. (2014). Natural variation in virulence of the entomopathogenic fungus *Beauveria bassiana* against malaria mosquitoes. *Malaria Journal*, 13(1), 479. <https://doi.org/10.1186/1475-2875-13-479>.
- van den Brule, T., Punt, M., Teertstra, W., Houbbraken, J., Wösten, H., & Dijksterhuis, J. (2020). The most heat-resistant conidia observed to date are formed by distinct strains of *Paecilomyces variotii*. *Environmental Microbiology*, 22(3), 986–999. <https://doi.org/10.1111/1462-2920.14791>.
- van Veluw, G. J., Teertstra, W. R., de Bekker, C., Vinck, A., van Beek, N., Muller, W. H., ... Wösten, H. A. B. (2013). Heterogeneity in liquid shaken cultures of *Aspergillus niger* inoculated with melanised conidia or conidia of pigmentation mutants. *Studies in Mycology*, 74(Supplement C), 47–57. <https://doi.org/10.3114/sim0008>.
- Wyatt, T. T., van Leeuwen, M. R., Golovina, E. A., Hoekstra, F. A., Kuenstner, E. J., Palumbo, E. A., ... Dijksterhuis, J. (2015). Functionality and prevalence of trehalose-based oligosaccharides as novel compatible solutes in ascospores of *Neosartorya fischeri* (*Aspergillus fischeri*) and other fungi. *Environmental Microbiology*, 17(2), 395–411. <https://doi.org/10.1111/1462-2920.12558>.
- Wyatt, T. T., Wosten, H. A., & Dijksterhuis, J. (2013). Fungal spores for dispersion in space and time. *Advances in Applied Microbiology*, 85, 43–91 2013/08/15 ed.
- Yilmaz, N., Visagie, C. M., Houbbraken, J., Frisvad, J. C., & Samson, R. A. (2014). Polyphasic taxonomy of the genus *Talaromyces*. *Studies in Mycology*, 78, 175–341. <https://doi.org/10.1016/j.simyco.2014.08.001>.